

Structure and Dynamics of Lanthanide Complexes of Triethylenetetramine-*N,N,N',N'',N''',N''''*-hexaacetic Acid (H_6ttha) and of Diamides $H_4ttha(NHR)$ Derived from H_6ttha as Studied by NMR, NMRD, and EPR

by Emrin Zitha-Bovens^{a)}, Robert N. Muller^{b)}, Sophie Laurent^{b)}, Luce Vander Elst^{b)}, Carlos F. G. C. Geraldes^{c)}, Herman van Bekkum^{a)}, and Joop A. Peters^{*a)}

^{a)} Laboratory for Applied Organic Chemistry and Catalysis, Delft University of Technology, Julianalaan 136, 2628 BL, Delft, The Netherlands (phone: +31 15 27 85892; e-mail: J.A.Peters@tnw.tudelft.nl)

^{b)} Department of Organic and Biomedical Chemistry, NMR and Molecular Imaging Laboratory, University of Mons-Hainaut, Avenue du champ de Mars 24, B-7000 Mons

^{c)} Departamento de Bioquímica, Faculdade de Ciências e Tecnologia, Universidade de Coimbra, Apartado 3126, P-3049 Coimbra

Dedicated to Professor *André E. Merbach* on the occasion of his 65th birthday

A multinuclear NMR study on $[Ln(ttha)]^{3-}$ and $[Ln\{ttha(NHR)_2\}]^-$ complexes ($R = Et, CH_2(CHOH)_4, CH_2OH$) shows that coordinating groups of the organic ligands in these complexes are occupying all coordination sites of the metal ions, leaving no space for coordination of H_2O molecules ($H_6ttha =$ triethylenetetramine-*N,N,N',N'',N''',N''''*-hexaacetic acid). The lanthanides of the first half of the series bind the ttha-type ligands in a decadentate fashion, while the complexes formed with the smaller ions of the second half of the lanthanide series are nonadentate. One carboxylate group of the ligand remains unbound in the latter complexes. In principle, the ttha complexes can exist in six enantiomeric forms. Only one of the pair of diastereoisomers can interconvert without decoordination of the ligand. This pair of isomers seems to be predominant in solution. For the $[Ln\{ttha(NHR)_2\}]^-$ complexes, the number of chiral centers is larger, resulting in 32 possible enantiomeric forms of the complexes. The NMR spectra of $[Nd\{ttha(NHEt)_2\}]^-$ indicate that two dynamic processes occur between the isomers in solution. The NMRD curves of $[Gd(ttha)]^{3-}$, $[Gd\{ttha(NHEt)_2\}]^-$, and $[Gd\{ttha(NHgluca)_2\}]^-$ ($NHgluca = D$ -glucamine) show significant differences with the previously determined outer-sphere contributions to the NMRD profiles of the corresponding $[Gd\{dtpa(NHR)_2\}]^-$ complexes, which can be ascribed to differences in the parameters determining the electronic relaxation.

1. Introduction. – Lanthanide complexes of polyaminopolycarboxylates have been studied intensively over the last decades because of their application as contrast agents for magnetic resonance imaging (MRI) [1]. Lanthanide complexes of ttha ($H_6ttha =$ triethylenetetramine-*N,N,N',N'',N''',N''''*-hexaacetic acid = 3,6,9,12-tetrakis(carboxymethyl)-3,6,9,12-tetraazatetradecanedioic acid), particularly $[Dy(ttha)]^{3-}$ and $[Tm(ttha)]^{3-}$, have also found applications as NMR-shift reagents for monovalent and divalent cations [2].

The complexes based on dtpa ($H_5dtpa =$ diethylenetriamine-*N,N,N',N''*-pentaacetic acid = *N,N*-bis{2-[bis(carboxymethyl)amino]ethyl}glycine) have been characterized in detail [1], while the ttha analogues have received far less attention. The various lanthanide complexes of ttha are not isostructural in solution. *Holz et al.* [3] have suggested different coordination modes for the $[La(ttha)]^{3-}$ and $[Lu(ttha)]^{3-}$ complexes. Also for the solid state, different coordination modes have been reported

for various lanthanide complexes of ttha [4–7]. The crystal structures show a ten- (La, Nd) or nine-fold (Gd, Dy) coordination geometry. This variation in coordination number can be ascribed to the lanthanide contraction along the series. Similar phenomena have been reported for Ln^{3+} complexes of other polyaminocarboxylates, e.g., of the egta ligand ($\text{H}_4\text{egta} = 3,12\text{-bis}(\text{carboxymethyl})\text{-}6,9\text{-dioxo-}3,12\text{-diazatetradecanedioic acid}$) [8].

The efficiency of MRI contrast agents [1] is generally expressed as the relaxivity, r_1 , which is the enhancement of the H_2O ^1H relaxation rate expressed in $\text{s}^{-1} \text{mM}^{-1}$. The relaxation-rate enhancement arises from: *i*) an inner-sphere contribution due to protons of H_2O molecules directly coordinated to the Gd^{3+} ion and in exchange with the bulk water, and *ii*) an outer-sphere contribution as a result of H_2O molecules freely diffusing along the paramagnetic center. Sometimes, a third contribution is considered, which is referred to as the second-sphere contribution [9]. It concerns H_2O molecules that are not directly coordinated to the Gd^{3+} ion but that are bound to the paramagnetic complex through, e.g., H-bonds. In the literature, there is general agreement that, for $[\text{Ln}(\text{ttha})]^{3-}$ complexes, the inner coordination sphere of the metal ion is fully occupied by donating groups of the ligand, leaving no space for the coordination of H_2O molecules. Consequently, the H_2O ^1H relaxation enhancement has no inner-sphere contribution; it is determined exclusively by the outer-sphere and the second-sphere relaxation. Therefore, the $[\text{Gd}(\text{ttha})]^{3-}$ complex is an interesting model to study these relaxation mechanisms.

Measurement of the magnetic-field dependence of the H_2O ^1H longitudinal relaxation rate as a function of the magnetic field (NMRD) is important for the evaluation of parameters governing the relaxivity of potential MRI contrast agents [1]. The $[\text{Gd}(\text{ttha})]^{3-}$ complex has been used as a model for the sum of the outer- and second-sphere contributions to the total relaxivity (r_1) of acyclic polyaminopolycarboxylates [10]. By subtracting the relaxivity of $[\text{Gd}(\text{ttha})]^{3-}$ from the observed r_1 of a Gd^{3+} complex of an acyclic polyaminopolycarboxylate, the inner-sphere contribution can be calculated, provided that the relaxivity of $[\text{Gd}(\text{ttha})]^{3-}$ is a reasonable estimation of outer-sphere and second-sphere relaxivity of the complex under investigation [10][11]. However, the NMRD data of $[\text{Gd}\{\text{dtpa}(\text{NHgluca})_2\}]$ ($\text{NHgluca} = \text{D-glucamine} = \text{D-glucos-}2,3,4,5,6\text{-pentahydroxyhexanamine}$) [12] could not be fitted with the *Solomon–Bloembergen–Morgan* equations [13–15] by using this estimation for the outer- and second-sphere contribution to the relaxivity [12]; so the question arises whether $[\text{Gd}(\text{ttha})]^{3-}$ is a suitable model for outer-sphere relaxation in Gd^{III} complexes of dtpa derivatives.

Here we report on an NMR and EPR study on the solution structures and dynamics of the lanthanide complexes of ttha and $\text{ttha}(\text{NHEt})_2$. The NMRD profiles of the Gd^{3+} complexes of ttha, $\text{ttha}(\text{NHEt})_2$, and $\text{ttha}(\text{NHgluca})_2$ (see *Fig. 1* for chemical structures) are analyzed and compared with literature data on the corresponding dtpa derivatives.

2. Results and Discussion. – 2.1. *Synthesis of the Ligands.* The diamide ligands $\text{H}_4\text{ttha}(\text{NHR})_2$ (derived from H_6ttha) used in this study (*Fig. 1*) were synthesized starting from H_6ttha . Heating a solution of this compound in Ac_2O and pyridine gave exclusively the dianhydride with the anhydride moieties at the terminal N-atoms.

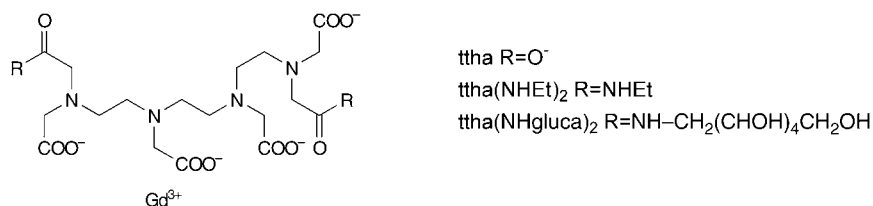


Fig. 1. Chemical structures of the ligands discussed

Reactions with the appropriate amines (ethanamine or D-glucamine) gave the diamides H₄ttha(NHET)₂ and H₄ttha(NHgluca)₂.

2.2. *Determination of the Hydration Number of the Lanthanide(III) Complexes.* Upon stepwise addition of DyCl₃ · 6 H₂O to an aqueous solution of H₆ttha, H₄ttha(NHET)₂, or H₄ttha(NHgluca)₂ at pH 6–6.5, the ¹⁷O-NMR chemical shift of H₂O hardly changed up to $\rho_L = 1$ ($\rho_L = [\text{Ln}^{3+}]/[\text{organic ligand}]$). At $\rho_L = 1$, the curve of $\delta(\text{O})$ vs. ρ_L showed a sudden break and at $\rho_L > 1$, the absolute value of $\delta(\text{O})$ of H₂O steeply increased. In that region, the $\delta(\text{O})$ of H₂O changed linearly with the concentration of the metal ion. These phenomena indicate that for all compounds, 1:1 Ln/ligand complexes are formed.

Previously, it has been shown that the lanthanide-induced shifts (LIS) for a Ln³⁺-bound O-atom are mainly of contact origin and that the hyperfine coupling constant does not vary significantly along the lanthanide series [16]. This may be exploited for the determination of the number of Ln³⁺-bound H₂O molecules (q) in the Ln³⁺ complexes, particularly for Ln = Dy³⁺, since for that ion, the contact contribution to the shift is predominant. From the induced shift of a solution of [Dy(D₂O)₈]³⁺, the LIS value at $\rho_w = 1$ ($\rho_w = [\text{Ln}^{3+}]/[\text{D}_2\text{O}]$) has been determined to be –19830 ppm. Therefore, the LIS value per Dy^{III}-bound H₂O is –2479 ppm (–19830/8), under the conditions applied. The initial slope of the LIS as a function of ρ_w (at $\rho_L < 1$) was close to zero for all ttha derivatives studied, indicating that no H₂O molecules are present in the first coordination sphere of the complexes of both ttha and ttha(NHR)₂. This is in agreement with previously reported X-ray structures, luminescence, and relaxivity studies on [Ln(ttha)]³⁻ complexes [3][7][17]. Table 1 compares the LIS of the water ¹⁷O-NMR resonance signals for several complexes of ttha derivatives with those of the corresponding dtpa complexes. The latter have one H₂O molecule in the inner coordination sphere, which is reflected in the much larger absolute LIS values. The small LIS that is measured for the ttha derivatives at $\rho_L = 1$ is originating from second- and outer-sphere H₂O molecules, and is of purely pseudo-contact origin. Since these H₂O molecules are located at a relatively large distance from the paramagnetic center and the pseudo-contact shift has a r^{-3} dependence on the distance, the resulting shift is rather small. Moreover, the H₂O molecules of the outer-sphere are not positioned on fixed locations with respect to the paramagnetic center and, therefore, induced shifts are averaged out.

The signs of the slopes of the titration curves at $\rho_L > 1$ correspond to the relative signs of the $\langle S_z \rangle$ values of the Ln³⁺ ions, which supports that the LIS value is mainly of contact origin (see Table 2). The slope of the LIS value of H₂O vs. ρ_w in the presence of

Table 1. Lanthanide-Induced Water ^{17}O -NMR Shifts [ppm] of LnL Complexes at $\rho_L = 1$

Ligand L	La ³⁺	Pr ³⁺	Nd ³⁺	Dy ³⁺	Tm ³⁺
dtpa ^{a)}	152	305	452	– 1983	177
ttha ^{b)}	0.60	8.26	13.05	– 0.95	5
ttha(NHEt) ₂ ^{b)}		0.44	0.32	– 0.32	– 0.04
ttha(NHgluca) ₂ ^{b)}		0.38	0.30	0.47	– 0.10

^{a)} [18]: pD = 7, T 73°. ^{b)} This study, pD 6–6.5, T = 75°.

an excess of Dy³⁺ ($\rho_L > 1$) is – 13408, which corresponds to an average of 5.4 H₂O molecules (– 13408 / – 2479) in the first coordination sphere of the Dy³⁺ ion. If there would be free Dy³⁺ present in solution, a slope corresponding to 8 H₂O molecules would be expected. Therefore, it may be concluded that the excess of Dy³⁺ is bound to the [Dy(ttha)]^{3–} complex. In the crystal structure of the bis(guanidinium) salt of [Dy(ttha)]^{3–} reported by *Ruloff et al.* [7], the ttha ligand is coordinated in a nine-fold coordination fashion through four N-atoms in the backbone and five of the carboxylate groups, whereas, one of the terminal acetate groups is not bound to the lanthanide ion. This uncoordinated carboxylate group might coordinate a second Dy³⁺ ion in the solution, which could explain the evaluated q -value for $\rho_L > 1$.

Table 2. Complexometric ^{17}O -NMR Titrations of LnL Complexes: Slopes of the Plots of δ [ppm] vs. ρ_w at $\rho_L > 1$, pD 6–6.5, T 75°.

Ligand L	Pr ³⁺	Nd ³⁺	Dy ³⁺	Tm ³⁺
ttha	–	–	– 13408	– 4688
ttha(NHEt) ₂	2427	3354	– 17928	– 3998
ttha(NHgluca) ₂	2033	2078	– 8919	– 2831

2.2. Elucidation of the Coordination Mode of the ttha and ttha(NHR)₂ Ligands by Means of ^{13}C -NMR. Upon stepwise addition of NdCl₃·6H₂O to a solution of 0.1M H₆ttha in D₂O at pH 6–6.5, a second set of signals appears in the ^{13}C -NMR spectrum, which indicates that the exchange between free and bound ligand is slow on the NMR time scale. Increase of the temperature to 80° did not result in coalescence of the resonances for free and bound ttha. Upon increase of ρ_L , the intensity of the new resonances increased at the expense of those of free ttha until at $\rho_L (= [\text{Nd}^{3+}]/[\text{L}]) = 1$, where the NMR spectrum showed only one set of signals. This supports the 1:1 Ln³⁺/ttha stoichiometry already concluded from the ^{17}O -NMR data. The number of signals that appeared in the spectrum at $\rho_L = 1$ indicates that several isomers of the lanthanide complex are formed in solution.

The ^{13}C -NMR spectrum of [Dy(ttha)]^{3–} could not be observed, probably due to extensive line broadening, which is typical for the heavier lanthanide ions [10][18][19]. The ^{13}C -NMR spectrum of the [Yb(ttha)]^{3–} complex was observable at 25° but it was very crowded with 14 resonances between 7 and 300 ppm, and no unambiguous peak assignments could be made. Therefore, we focused our attention on the Nd³⁺ complexes.

The ^{13}C -NMR spectrum of the $[\text{Nd}(\text{ttha})]^{3-}$ complex at 60° exhibited three sets of three signals for the carboxylate, acetate, and ethylene (=ethane-1,2-diyl) C-atoms, respectively (Fig. 2). This implies the presence of a 'pseudo' mirror plane in the complex that can be due to a rapid rearrangement of the ttha ligand. The integrals of the three carboxylate signals were comparable, which is consistent with the existence of such a 'pseudo' mirror plane. After addition of MeOH to the sample and cooling to -10° , the signals broadened. Further cooling to -30° led to splitting into at least six resonances in the carboxylate region (Fig. 2), indicating that the motion is frozen out at this temperature. From the coalescence temperature (-10°), the ΔG^\ddagger value for the exchange process was calculated to be $50 \text{ kJ}\cdot\text{mol}^{-1}$. Referring to previous work on structure elucidation of analogous lanthanide complexes [19], an exchange process characterized by a ΔG^\ddagger value of this magnitude suggests that it is related to 'wagging' of the ethylenediamine backbone. This so-called 'wagging motion' involves the racemi-

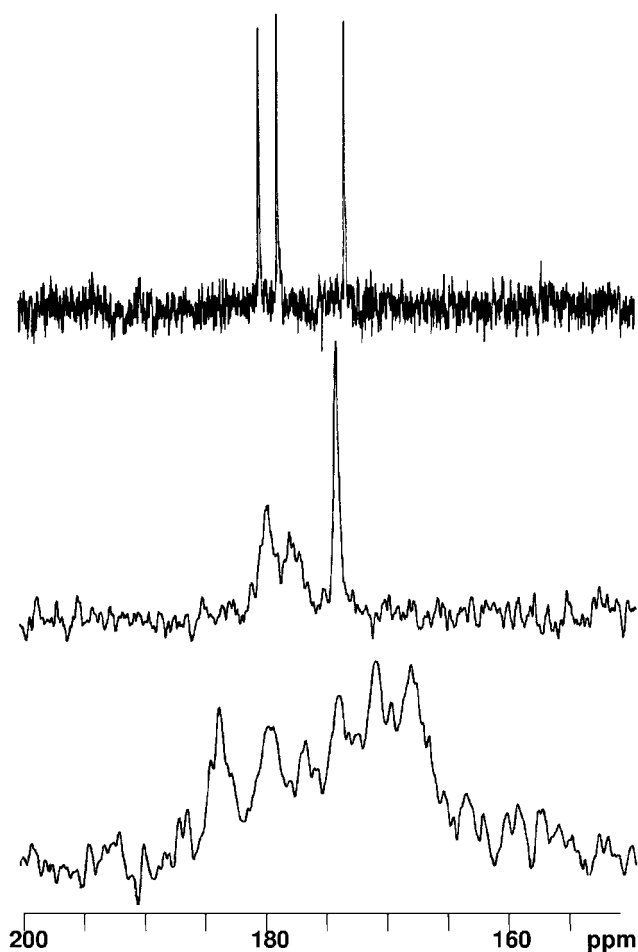


Fig. 2. NMR Spectra of the carboxylate region of $[\text{Nd}(\text{ttha})]^{3-}$ at 60° (top), -10° (middle), and -30° (bottom)

zation of the two *gauche* conformations (λ and δ) of Ln³⁺-bound ethylenediamine bridges.

The ¹³C-NMR spectra of [Nd{ttha(NHEt)₂}]⁻ and [Nd{ttha(NHgluca)₂}]⁻ at pH 6–6.5 are much more complex. The carboxylate region of the ttha(NHEt)₂ complex exhibits at least 16 resonances. As a consequence, a detailed peak assignment is impossible, and only groups of signals (*e.g.*, carboxylate, acetate, or ethylene C-signals) were identified. These ¹³C-NMR spectra indicate that the [Nd{ttha(NHR)₂}]⁻ complexes occur in several isomeric forms. An analysis of the possible isomers that can be formed in solution and the dynamic processes that can occur between these isomers is given below.

To determine the distances between the various C-atoms in the ligand and the lanthanide ion, ¹³C longitudinal relaxation time (*T*₁) measurements were performed. Among the lighter Ln³⁺ ions, Nd³⁺ has the longest electronic relaxation times, so this ion is favorable for these studies. The ¹³C longitudinal relaxation rates for the [Nd(ttha)]³⁻ complex were determined at 60°. At this temperature, the species in solution are in the fast-exchange regime on the NMR time scale, which resulted in relatively simple spectra (see above). For [Nd{ttha(NHEt)₂}]⁻ the longitudinal relaxation times were determined at 25° and at a relatively high concentration (0.4M). As was mentioned in the previous paragraph, the ¹³C-NMR spectrum of this complex is rather crowded due to the presence of various isomers in solution. The longitudinal relaxation rates of the various ¹³C nuclei in the Nd³⁺ complex were corrected for the diamagnetic contribution by subtraction of their respective relaxation rates in the La³⁺ complex at the same temperature. The data obtained are compiled in Table 3.

Table 3. ¹³C-NMR 1/*T*₁ Relaxation Rates [s⁻¹] of LnL Complexes (at 75.5 MHz)

Ligand L	C-Atom	Nd ³⁺ complex	La ³⁺ complex
ttha ^{a)}	CO	7.01–8.03	0.14–0.16
	CH ₂ CO	7.38–10.22	2.19–2.43
	CH ₂ CH ₂	7.54–9.63	2.63–2.89
ttha(NHEt) ₂ ^{b)}	CO	9.25–14.98	0.70–0.92

^{a)} 0.1M, 60°. ^{b)} 0.4M, 25°.

Since various isomers exist in solution, the relaxation rates obtained are weighted averages for the individual isomers. Two relaxation mechanisms are of importance in this case: the ‘classical’ dipolar relaxation ($1/T_{1,\text{dip}}$) [13–15] and the *Curie* relaxation ($1/T_{1,\text{Curie}}$) [20][21]. *Eqns. 1* and *2* give the contributions of these mechanisms, respectively, where $\mu_0/4\pi$ is the magnetic permeability of a vacuum, γ_1 is the magnetogyric ratio of ¹³C, μ_{eff} is the effective moment of Nd^{III}, β is the *Bohr* magneton, r is the distance between the nucleus under study and Nd^{III}, H_0 is the magnetic field strength, and τ_R is the rotational correlation time of the Nd^{III} complex. If it is assumed that the magnitude of the rotational correlation time (τ_R) of the compounds under study is between 60 and 300 ps, then it can be calculated *via Eqns. 1* and *2* that the *Curie* contribution to the total relaxation is between 8 and 30%, under the conditions applied. We decided to neglect this contribution for the calculation of Nd–C distances, since, as

a result of the r^{-6} relationship, this leads to an error in the distances of less than 4%.

$$\frac{1}{T_{1,\text{dip}}} = \frac{4}{3} \left(\frac{\mu_0}{4\pi} \right)^2 \frac{\gamma_1^2 \mu_{\text{eff}}^2 \beta^2}{r^6} T_{1e} \quad (1)$$

$$\frac{1}{T_{1,\text{Curie}}} = \frac{6}{5} \left(\frac{\gamma_1^2 H_0^2 \mu_{\text{eff}}^4 \beta^4}{(3kT)^2 r^6} \right) \left(\frac{\tau_R}{1 + \omega_1^2 \tau_R^2} \right) \quad (2)$$

By use of the data reported by *Alsaadi et al.*, the longitudinal electronic relaxation time, T_{1e} , for Nd^{3+} complexes at 60° is estimated to be $1.74 \cdot 10^{-13}$ s [22][23]. The distances as determined with *Eqn. 1* are summarized in *Table 4*. A comparison is made with the average distances in the crystal structures of $[\text{Nd}(\text{ttha})]^{3-}$ and $[\text{Dy}(\text{ttha})]^{3-}$ described respectively by *Mondry et al.* [5] and *Ruloff et al.* [7]. In the crystals of the Nd complex [5], the ligand is coordinated to the metal ion in a decadentate fashion *via* the four N-atoms of the ethylenetriamine backbone and six carboxylate O-atoms, whereas the corresponding Dy^{3+} complex [7] has one of the acetate groups uncoordinated. Since the average distances of the three carboxylate resonances as determined from the relaxation rates are about the same and in good agreement with those in the crystal structure of $[\text{Nd}(\text{ttha})]^{3-}$, it can be concluded that the solution-state structure of $[\text{Nd}(\text{ttha})]^{3-}$ is comparable to that in the solid state. If one of the carboxylate groups would not have been bound to the Nd^{3+} ion (as in the structure of $[\text{Dy}(\text{ttha})]^{3-}$ in the solid state), its distance to the Nd^{3+} ion would have been *ca.* 4.9 Å rather than *ca.* 3.4 Å. A significantly larger relaxation rate would have been obtained for the concerning resonance, even if it is taken into account that exchange of unbound and bound carboxylates may occur.

Table 4. *Ln–C Distances [Å] in $[\text{Nd}(\text{ttha})]^{3-}$ and $[\text{Nd}\{\text{ttha}(\text{NHEt})_2\}]^-$ from ^{13}C -NMR T_1 Analysis and Comparison with Crystal Structure Data and NMR Data of a *dtpa* Analogue*

	CO	CH ₂ CO	CH ₂ CH ₂
$[\text{Nd}(\text{ttha})]^{3-}$ (NMR) ^a	3.48, 3.48, 3.40	3.40, 3.68, 3.47	3.63, 3.50, 3.72
$[\text{Nd}(\text{ttha})]^{3-}$ (X-ray) ^b	3.36 ± 0.06	3.51 ± 0.05	3.55 ± 0.07
$[\text{Dy}(\text{ttha})]^{3-}$ (X-ray) ^c	3.25 ± 0.03 , 4.90	3.40 ± 0.07	3.47 ± 0.07
$[\text{Nd}\{\text{ttha}(\text{NHEt})_2\}]^-$ (NMR) ^a	3.00–3.26		
$[\text{Nd}\{\text{dtpa}(\text{NHPr})_2\}]$ (NMR) ^d	3.08–3.19	3.25–3.37	3.36–3.43

^a) This work. ^b) Measured from model based on crystal coordinates reported by *Mondry et al.* [5]. ^c) Measured from model based on crystal coordinates reported by *Ruloff et al.* [7]. ^d) [18]; $\text{H}_3\text{dtpa}(\text{NHPr})_2 = N,N'$ -bis[2-oxo-2-propylamino]ethyl]diethylenetriamine- N,N',N'' -triacetic acid.

The distances that were obtained for carbonyl C-atoms in the $[\text{Nd}\{\text{ttha}(\text{NHEt})_2\}]^-$ complex were similar to those reported previously for $[\text{Nd}\{\text{dtpa}(\text{NHR})_2\}]$ complexes [19], suggesting that the coordination mode is similar (binding of the Nd^{3+} ion *via* four N atoms of the ttha backbone, four carboxylate O-atoms, and two amide O-atoms). Unfortunately, the crowding in the ^{13}C -NMR spectra of $[\text{Nd}\{\text{ttha}(\text{NHEt})_2\}]^-$ did not allow the determination of the T_1 values for the other resonances.

2.3. *Isomers of the Ln^{3+} Complexes of ttha and ttha(NHR)₂*. The results of the ^{13}C relaxation rate measurements (see above) indicate decadentate coordination of the

ttha ligand with Nd^{3+} through the four N-atoms of the ethylenediamine backbone and six O-atoms of the carboxylate groups. We assume that, also in solution, the complexes with the heavier Ln^{3+} ions will have nonadentate coordination, with one of the acetate groups not bound to the Ln^{3+} ion. This would be in line with previous ^1H - and ^{13}C -NMR studies of Holz and Horrocks [3] on the diamagnetic La^{3+} , Lu^{3+} , and Y^{3+} complexes of ttha. Assignments could not be made due to fluxional processes. The spectra of the Lu^{3+} and Y^{3+} complexes showed nine and ten resonances, respectively, in the carboxylate C-region. The NMR spectrum of the La^{3+} complex was similar to the spectra of the Nd^{3+} complex at high temperature ($>60^\circ$) described above and consisted of three carboxylate, three acetate and three ethylene signals.

Upon binding in either a nine- or a ten-coordinate fashion, the inversion of the N-atoms is precluded and, therefore, N(2) and N(3) (for labeling of atoms, see Fig. 3) are chiral. Furthermore, it is remarkable that in crystal structures of the $[\text{Ln}(\text{ttha})]^{3-}$ complexes, the ethylene units in the triethylenetetramine backbone occur exclusively in the $\lambda\lambda\delta$ or $\delta\delta\lambda$ conformation. The ethylenediamine bridge that has a opposing conformation is in all cases carrying the carboxylate group that is characterized by a longer binding distance towards the lanthanide ion (ten-fold coordination) or that is not bound at all (nine-fold coordination). For the complexes with the ttha ligand bound in a 9-coordinate fashion, the N-atom carrying the uncoordinated acetate function is chiral as well. We assume, however, that a rapid coordination-decoordination process effectively produces a racemization with respect to this N-atom. If we furthermore assume that the ethylene bridges can occur in $\lambda\lambda\delta$ or $\delta\delta\lambda$ conformations, at most eight enantiomeric forms can be expected for a $[\text{Ln}(\text{ttha})]^{3-}$ complex. However, an inspection of Dreiding models shows that the ttha ligand can be wrapped around a Ln^{3+} ion in only six different ways, one of the diastereomeric pairs is impossible to form for steric reasons. In Fig. 3, the possible isomers are depicted schematically, assuming nine-coordination in a tricapped trigonal prism. Similar structures can be envisaged for ten-coordination. The labels in Fig. 3, (S,S), (R,R), (S,R), and (R,S), describe the arrangement of the substituents on N(2) and N(3).

The six isomers are three pairs of mirror images, **1** and **1'**, **2** and **2'**, and **3** and **3'**. Only the latter pair of isomers, **3** and **3'** i.e., (S,R) and (R,S) can interconvert without decoordination. The interconversion from (R,R) to (S,S) always requires decoordination of N(2) or N(3). For dtpa (and $\text{dtpa}(\text{NHR})_2$), this (R,S)/(S,R) interconversion is possible via the so-called 'wagging motion' that results in the racemization of the central N-atom. Inspection of molecular models indicates that the wagging motion as such is not possible for the ttha ligand. The ^{13}C -NMR spectrum of $[\text{Nd}(\text{ttha})]^{3-}$ described above suggests that one of the three possible diastereoisomeric pairs is predominant, since the spectrum at low temperature shows only one set of signals for each C-atom in the complex. The exchange process observed between these isomers with a ΔG^\ddagger value of $50 \text{ kJ} \cdot \text{mol}^{-1}$ (see above) indicates that these isomers can be assigned to (R,S) and (S,R), i.e., to **3** and **3'**. Exchange between isomers involving decoordination of terminal N-atoms and the adjacent acetate groups would have a ΔG^\ddagger value of ca. $70 \text{ kJ} \cdot \text{mol}^{-1}$ [19].

A variable-temperature ^{13}C -NMR study on the $[\text{Nd}\{\text{ttha}(\text{NHEt})_2\}]^-$ complex provided more-complicated spectra. The situation in case of the $\text{ttha}(\text{NHEt})_2$ complexes is much more complicated because the terminal N-atoms are also chiral

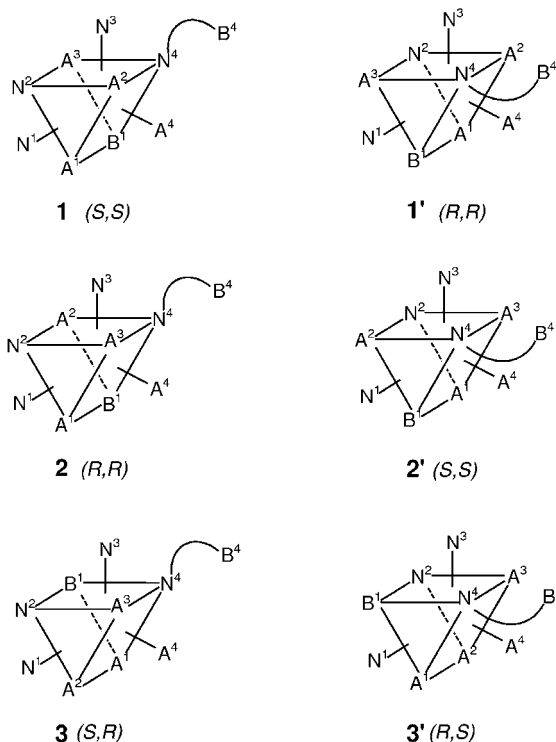
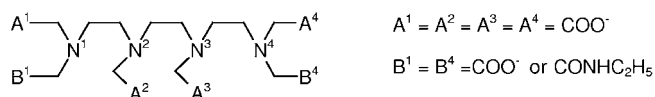


Fig. 3. Coordination geometries for $[\text{Ln}(\text{ttha})]^{3-}$ complexes

upon coordination, so four times as many isomers ($8 \cdot 4 = 32$, or 16 diastereomeric pairs) can be formed in solution. The occurrence of various isomers is confirmed by the ^{13}C -NMR spectrum at 25° , which showed at least 16 signals in the carboxylate region. At 80° , some of these signals remained sharp while others had broadened and almost disappeared in the base line. So probably two dynamic processes occur between the isomers, one is relatively fast and the other is much slower, and most likely involves partial decoordination of the ligand. Previously, similar exchange processes have been observed in the $[\text{Ln}\{\text{dtpa}(\text{NHR})_2\}]$ complexes [12][19]. However, the number of different species of Ln^{3+} complexes of ttha or its derivatives that can be formed in aqueous solution has strongly increased with respect to the corresponding dtpa derivatives [12][19].

2.4. *Determination of the Location of Counter-Ions.* Because of its very small quadrupolar moment, ^6Li has a slow quadrupolar relaxation and, therefore, is a very

suitable probe for studying the location of counter-ions of negatively charged Ln^{3+} complexes [24]. The longitudinal relaxation rate ($1/T_1$) was measured in a solution of 0.1M $[\text{Li}_6(\text{ttha})]$ and Nd^{3+} at $\rho = 0.95$ in D_2O at pH 6.5 and at 60° . For the calculation of the longitudinal relaxation rate, it was assumed that all Nd^{3+} was present as $\text{Li}_3[\text{Nd}(\text{ttha})]$. This implies that half of the Li^+ ions are bound to the $[\text{Nd}(\text{ttha})]^{3-}$ complex. The ‘bound’ counter-ions are in fast exchange on the NMR timescale with the ‘free’ Li^+ ions. If it is assumed that the relaxation rate of free Li^+ is negligible [24], the longitudinal relaxation rate of the Li^+ ions in the $[\text{Li}_3[\text{Nd}(\text{ttha})]]$ is calculated to be 0.085 s^{-1} .

By using *Eqn. 1* and the estimated value for $T_{1e} = 1.74 \cdot 10^{-13}$ at 60° , a $\text{Nd}^{3+}-\text{Li}^+$ distance of 6.8 \AA was calculated. This $\text{Nd}^{3+}-\text{Li}^+$ distance is slightly larger than the value determined for the analogous dtpa complex ($r_{\text{Nd}-\text{Li}} = 5.6 \text{ \AA}$) [18], which can be explained by the larger radius of the $\text{Li}_3[\text{Nd}(\text{ttha})]$ complex.

2.5. NMRD Profiles. The NMRD profiles of the $[\text{Gd}(\text{ttha})]^{3-}$, $[\text{Gd}\{\text{ttha}(\text{NHET})_2\}]^-$, and $[\text{Gd}\{\text{ttha}(\text{NHgluca})_2\}]^-$ complexes were recorded at different temperatures ($5, 15, 25, 37, \text{ and } 45^\circ$). The profiles show significant differences (see *Fig. 4*), indicating that the profile of $[\text{Gd}(\text{ttha})]^{3-}$ cannot be used as general model for the outer-sphere contribution to the relaxivity of Gd^{3+} complexes of acyclic polyaminocarboxylates.

From the magnetic-field dependence of the H_2O proton $1/T_1$ longitudinal relaxation times, induced by the paramagnetic Gd^{3+} ion, several parameters that govern the relaxivity were evaluated by fitting the experimental data to the outer-sphere relaxation model as described by *Freed (Eqns. 3 and 4)* [25], where N_A is *Avogadro's* number, a_{GdH} is the distance of closest approach of the H_2O molecule to Gd^{III} , and τ_{GdH} is the correlation time corresponding with $a_{\text{GdH}}^2/D_{\text{GdH}}$. D_{GdH} stands for the diffusion coefficient. The spectral density functions, $J_{\text{OS}}(\omega_1, T_{je})$ ($j = 1, 2$) in *Eqn. 4*, express the electronic-relaxation dependence, ω_1 is the nuclear *Larmor* frequency, and T_{je} are the electronic relaxation times, which are described by the *Solomon–Bloembergen–Morgan* theory [13–15]. In this case, the semi-empirical equations proposed by *Merbach* and co-workers were applied (*Eqns. 5–8*) [26]. Here, τ_v is the correlation time of the modulation of the zero-field splitting, $1/T_{\text{eSr}}$ is a correction for the so-called spin-rotation mechanism, and τ_R is the rotation correlation time. Although the *Solomon–Bloembergen–Morgan* theory is oversimplified [27][28], it generally adequately describes NMRD profiles, and it has the advantage of its simplicity.

$$r^{\text{OS}} = \left(\frac{32\pi}{405}\right) \left(\frac{\mu_0}{4\pi}\right)^2 \gamma_1^2 \gamma_S^2 \hbar^2 S(S+1) \frac{N_A}{a_{\text{GdH}} D_{\text{GdH}}} [3J_{\text{OS}}(\omega_1, T_{1e}) + 7J_{\text{OS}}(\omega_S, T_{1e})] \quad (3)$$

$$J_{\text{OS}}(\omega, T_{je}) =$$

$$\text{Re} \left\{ \frac{1 + \frac{1}{4} \left[i\omega\tau_{\text{GdH}} + \left(\frac{\tau_{\text{GdH}}}{T_{je}}\right) \right]^{\frac{1}{2}}}{1 + \left[i\omega\tau_{\text{GdH}} + \left(\frac{\tau_{\text{GdH}}}{T_{je}}\right) \right]^{\frac{1}{2}} + \frac{4}{9} \left[i\omega\tau_{\text{GdH}} + \left(\frac{\tau_{\text{GdH}}}{T_{je}}\right) \right] + \frac{1}{9} \left[i\omega\tau_{\text{GdH}} + \left(\frac{\tau_{\text{GdH}}}{T_{je}}\right) \right]^{\frac{3}{2}}} \right\} \quad (4)$$

$$\frac{1}{T_{1e}} = \frac{1}{25} \Delta^2 \tau_v [4S(S+1) - 3] \left(\frac{1}{1 + \omega_s^2 \tau_v^2} + \frac{4}{1 + 4\omega_s^2 \tau_v^2} \right) + \frac{1}{T_{eSr}} \quad (5)$$

$$\frac{1}{T_{2e}} = \Delta^2 \tau_v \left(\frac{5.26}{1 + 0.372\omega_s^2 \tau_v^2} + \frac{7.18}{1 + 1.24\omega_s \tau_v} \right) + \frac{1}{T_{eSr}} \quad (6)$$

$$\frac{1}{T_{eSr}} = \frac{\delta g_L^2}{9\tau_R} \quad (7)$$

To limit the number of variables in the fitting procedure, diffusion coefficients of the different Ln^{3+} complexes were estimated by the recently derived semi-empirical Eqn. 8 [29]. Here M_r is the molecular weight (= relative molar mass) of the complex under study. The value of the distance of closest approach of H_2O protons to Gd^{3+} (a_{GdH}) was fixed at 3.5 Å, the same value as applied in previous studies on dtpa derivatives [12][30]. Good fits were obtained by using this model (see Fig. 4). In Table 5, the best-fit parameters are compared with reported values for corresponding dtpa compounds. The values of τ_v , the correlation time for modulation of the zero-field splitting that were found for the Gd^{3+} complexes of the ttha type of ligands are significantly smaller than those of corresponding dtpa ligands [11][26] (see Table 5). The zero-field limiting values of the electronic relaxation times, τ_{s0} , were calculated from τ_v , and the mean-square of the zero-field splitting interaction, Δ^2 , by using the relation $\tau_{s0} = (12\Delta^2\tau_v)^{-1}$. The electronic relaxation time of $[\text{Gd}(\text{ttha})]^{3-}$ is significantly larger than that of $[\text{Gd}(\text{dtpa})]^-$, which may be ascribed to the relative rigidity of the ttha complex as a result of the complete encapsulation of the paramagnetic center by the ligand molecule.

$$D_{\text{GdH}} = 2.17 \cdot 10^{-9} + \frac{3.97 \cdot 10^{-8}}{M_r} + \frac{1.01 \cdot 10^{-4}}{M_r^2} \quad (8)$$

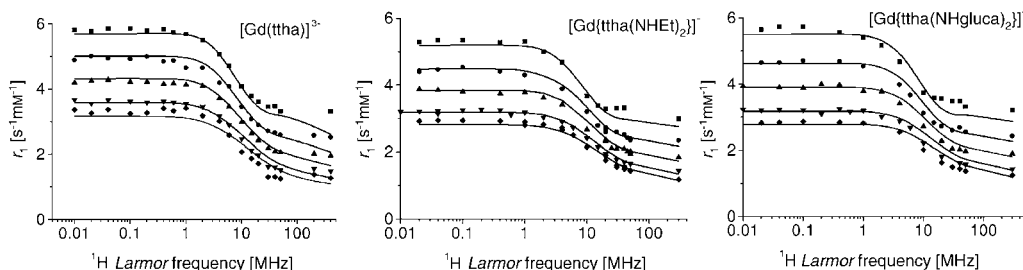


Fig. 4. NMRD Profiles of $[\text{Gd}(\text{ttha})]^{3-}$, $[\text{Gd}(\text{ttha}(\text{NHET})_2)]^-$, and $[\text{Gd}(\text{ttha}(\text{NHgluca})_2)]^-$ with best fit curves (see text) at 5 (■), 15 (●), 25 (▲), 37 (▼), and 45° (◆)

A second set of fittings of the NMRD profiles was performed with a model in which a second-sphere contribution was included. This contribution was calculated analogously to the well-known procedures for the calculation of the inner-sphere

Table 5. Results of NMRD Fittings, Comparison with Parameters Reported for Gd^{3+} Complexes of dtpa Derivatives ^{a)}

	dtpa ^{b)}	dtpa(NHMe) ₂ ^{b)}	dtpa(NHgluca) ₂ ^{c)}	ttha ^{d)}	ttha(NHEt) ₂ ^{c)}	ttha(NHgluca) ₂ ^{c)}			
q_{ss}	0	0	0	0	1.6 ± 0.6	0	0.9 ± 0.4	0	2.1 ± 0.3
τ_v^{298} [ps]	25 ± 1	25 ± 1	14 ± 1	9 ± 1	7 ± 1	8.0 ± 0.5	10 ± 1	9 ± 1	11 ± 1
E_v [kJ/mol]	1.6 ± 1.8	3.9 ± 1.4	1.1 ± 1.7	15 ± 2	19 ± 2	6 ± 1	11 ± 2	1 ± 1	12 ± 2
Δ^2 [10^{20} s ⁻²]	0.46 ± 0.02	0.41 ± 0.02	0.63 ± 0.08	0.66 ± 0.07	0.89 ± 0.22	1.26 ± 0.07	0.90 ± 0.15	1.26 ± 0.12	0.66 ± 0.13
τ_{SO}^{298} [ps]	72	81	94	141	126	82	97	77	103
D_{GdH}^{298} [10^{-10} m ² s ⁻¹]	20 ± 3	23 ± 2	26 ± 2	24.6 ^{e)}	24.6 ^{e)}	24.2 ^{e)}	24.2 ^{e)}	23.1 ^{e)}	23.1 ^{e)}
E_{DGdH} [kJ mol ⁻¹]	19.4 ± 1.8	12.9 ± 2.1	20.5 ± 1.6	18.2	18.2	18.2	18.2	18.2	18.2
a_{GdH} [Å]	3.5	3.5	3.5	3.5	3.68 ± 0.09	3.5	3.73 ± 0.05	3.5	4.13 ± 0.08

^{a)} The values in italics were fixed during the fitting procedure. E_v and E_{DGdH} are the activation energies for τ_v and D_{GdH} , respectively. ^{b)} [30]. ^{c)} [12]. ^{d)} This work. ^{e)} Estimated with Eqn. 8.

contribution [1]. It is difficult to evaluate the second-sphere parameters because a strong correlation exists among various parameters. The distance of the second-sphere H₂O molecules was fixed at 4.1 Å and their residence time in the second coordination sphere at 25 ps [31]. The rotational correlation time τ_R was estimated from that of [Gd(dtpa)]²⁻ [30] by using a correction for the difference in molecular volume as determined from molecular models. Furthermore, the parameter δ_{gL}^2 was fixed at 0.021. Keeping a_{GdH} fixed at 3.5 Å resulted in optimal fits for the number of second-sphere H₂O molecules, q_{ss} , close to zero. Only upon treating a_{GdH} as an adjustable parameter optimal fits with non-zero q_{ss} values ($q_{ss} = 1-2$, see Table 5) and somewhat higher a_{GdH} values (3.7–4.1 Å) were obtained. However, the goodness-of-fit did not improve upon inclusion of the second-sphere contribution to the relaxivity.

2.6. EPR Measurements. The X-band (0.34 T) EPR spectra of [Gd(dtpa)]²⁻, [Gd{dtpa(NHMe)₂}], [Gd{dtpa(NHCH₂Ph)}], [Gd(ttha)]³⁻, and [Gd{ttha(NHCH₂Ph)}]⁻ showed approximately Lorentzian lines of $g \approx 2$. The EPR spectra of [Gd(dtpa)]²⁻, [Gd{dtpa(NHMe)₂}] were in good agreement with those reported by *Merbach* and co-workers [30]. The transverse electronic relaxation times were calculated from the peak-to-peak line widths, ΔH_{pp} , with Eqn. 9, where g_L is the Landé g factor. The results obtained are compiled in Table 6 and compared with the T_{2e} values evaluated from the fittings of the NMRD profiles. The line width of resonance of [Gd(ttha)]³⁻ was remarkably narrow indicating a relatively long relaxation time for this complex, which is in good agreement with the results obtained from the fitting of the NMRD profile with the model without second-sphere H₂O molecules. However, the EPR data of the diamide derivatives agree slightly better with the NMRD parameters for a model that includes one to two second-sphere H₂O molecules.

$$T_{2e} = \frac{2\hbar}{g_L \beta \Delta H_{pp} \sqrt{3}} \quad (9)$$

It may be concluded that the parameters governing the electronic relaxation of Gd³⁺ complexes are too sensitive to structural changes to allow use of the NMRD profile of [Gd(ttha)]³⁻ (or other complexes that have no inner-sphere H₂O molecules)

Table 6. Linewidths in X-Band EPR Spectra of Gd^{III} Complexes of dtpa, ttha, and Some of Their Diamides at 25° and pH 7

	ΔH_{pp} [G]	$T_{2c}(\text{exp})$ [ps]	$T_{2c}(\text{calc})$ [ps] ^{a)}
[Gd(dtpa)] ²⁻	560 ± 50	117 ± 10	
[Gd{dtpa(NHMe) ₂ }	420 ± 50	156 ± 19	
[Gd{dtpa(NHBu) ₂ }	415 ± 50	158 ± 19	
[Gd(ttha)] ³⁻	280 ± 50	234 ± 42	211 ($q_{ss} = 0$); 157 ($q_{ss} = 1.6$)
[Gd{ttha(NHBu) ₂ }] ⁻	350 ± 50	187 ± 27	104 ($q_{ss} = 0$); 130 ($q_{ss} = 0.9$) ^{b)}

^{a)} Calculated with the best-fit parameters given in Table 5. ^{b)} Values for [Gd{ttha(NHEt)₂}]⁻.

as a general model for the outer- and second-sphere contributions. The present study also shows that the NMRD profiles can be adequately fit with a model that does not take into account a second-sphere contribution. However, a small contribution of a few second-sphere H₂O molecules cannot be excluded on the basis of the present results.

Previously, *Chen et al.* have suggested that the second-sphere contributes more than 30% of the relaxivity of [Gd(ttha)]³⁻ [32]. These authors have fit their data with the value of a_{GdH} fixed at 4.4 Å, which results in a considerably lower calculated outer-sphere contribution than in the present study, where we used $a_{\text{GdH}} = 3.5 - 3.7$ Å. This is compensated by a large second-sphere contribution and by a relatively low best-fit value of τ_{s0} of 81.5 ps. The latter value does not agree with that obtained in the present study (126–141 ps), which is supported by the EPR data.

The support and sponsorship concerted by *COST Action D18 'Lanthanide Chemistry for Diagnosis and Therapy'* are kindly acknowledged. *C.F.G.C.G.* thanks *Giovannia A. Pereira* for help in performing the EPR experiments and acknowledges financial support from the *F.C.T.*, Portugal (project POCTI/QUI/47005/2002), and *FEDER*. *R. N. M.*, *S. L.* and *L. V. E.* thank the *FNRS* and the *ARC Program 00/05-258* of the French Community of Belgium.

Experimental Part

General. All chemicals used were purchased from *Acros* or *Aldrich* and were used without further purification. A color test reaction for free lanthanides was performed with *Arsenazo III* as the indicator [33]. pH Measurements were made at r.t. with a *Corning 125* pH meter and a calibrated micro-combination probe purchased from *Aldrich Chemical Co.* The pH values given are direct meter readings; no correction was made for the deuterium isotope effect. Membrane filtrations were performed at neutral pH under 20 bar N₂ pressure over a *Toray Romembra®-UTC-60* membrane, *Toray Industries Inc.*, Tokyo, Japan.

N,N'-Ethane-1,2-diylbis[N-[2-(2,6-dioxomorpholin-4-yl)ethyl]glycine (H₂ttha-dianhydride). A suspension of H₄ttha (25 g, 50 mmol) in Ac₂O (19 ml, 200 mmol) and pyridine (24 ml) was stirred for 24 h at 65°. The brownish solid obtained was filtered and washed with dry Et₂O and then dried overnight under vacuum: 17.6 g, 76.6%) H₂ttha-dianhydride. ¹³C-NMR (100.6 MHz, (D₆)DMSO): 172.3; 170.4; 55.0; 54.6; 51.4; 50.4.

6,9-Bis(carboxymethyl)-3,12-bis[2-(ethylamino)-2-oxoethyl]-3,6,9,12-tetraazatetradecanedioic acid (H₄ttha(NHEt)₂). A mixture of DBN (=1,5-diazabicyclo[4.3.0]non-5-ene; 2 ml), DMSO (200 ml), and ethanamine (70% in H₂O; 3.1 g, 68 mmol) was heated at 50°. Then, H₂ttha-dianhydride (6.5 g, 14.2 mmol) was added in small portions within 30 min. The mixture was stirred for 4 h and subsequently evaporated. The brownish oil obtained was diluted with H₂O (15 ml) and brought to pH 10.5 with 4M NaOH. This soln. was purified by ion-exchange chromatography (*Dowex-OAc*⁻, O → 3M AcOH gradient). The fractions were analyzed by ¹³C-NMR. The combined aq. fractions containing pure product were neutralized (pH 7) and then desalted *via* membrane filtration. Lyophilization gave H₄ttha(NHEt)₂. (1.78 g, 22.5%). Yellow-brownish solid. ¹³C-NMR (100.6 MHz, D₂O, pH 1.5): 174.0; 173.4; 169.8; 58.5; 57.9; 56.5; 53.4; 53.0; 52.4; 36.0; 15.0.

3,12-Bis[2-(D-glucosyl)-2-oxoethyl]-6,9-bis(carboxymethyl)-3,6,9,12-tetraazatetradecanedioic Acid (H₄ttha(NHgluca)₂). To a soln. of (+)-D-glucamine (12.8 g, 70.7 mmol) in DMSO

(175 ml) containing DBN (1 ml), H₂thta-dianhydride (6.5 g, 14.2 mmol) was added in small portions, and the red-brown mixture was stirred overnight at 50°. After concentration, a dark oil was obtained that was diluted with H₂O (15 ml). The pH was brought to 2.5 with 2M aq. HCl soln., and the soln. obtained was purified by ion-exchange chromatography (Dowex-H⁺, 0 → 2M HCl gradient). After ¹³C-NMR analysis, the pH of the combined aq. fractions containing pure product was adjusted to 8, and then the salts were removed *via* membrane filtration. Lyophilization gave H₂thta(NHgluca)₂ (7.6 g, 55%). Pale yellow solid. ¹³C-NMR (100.6 MHz, D₂O, pH 12): 181.0; 180.6; 180.4; 175.9; 175.7; 73.3; 73.2; 72.7; 72.6; 71.6; 64.3; 60.5; 59.7; 53.7; 53.1; 52.8; 43.6; 43.2; 23.4.

NMR Measurements. ¹H-, ⁶Li-, ¹³C-, and ¹⁷O-NMR Spectra: Varian Unity-300 or Varian VXR-400-S spectrometer, ¹H and ¹³C spectra, *t*-BuOH as internal standard (¹H signal at 1.2 ppm, Me ¹³C signal at 31.2 ppm); ¹⁷O spectra, D₂O as external reference and determination of δ by fitting the observed signal with a Lorentzian line function; ⁶Li spectra were recorded without lock to prevent interference with the lock frequency.

NMRD Measurements. The 1/*T*₁ NMR dispersion (NMRD) profiles of the H₂O protons were recorded at several temperatures on an IBM Research Relaxometer at the University of Mons-Hainaut (Belgium), by using the field-cycling method and covering a continuum of magnetic fields from 2.5 · 10⁻⁴ T to 1.2 T (corresponding to a Larmor-frequency range of 0.01–50 MHz). The absolute uncertainty in the measured 1/*T*₁ for the NMRD measurements was ±3%. The longitudinal ¹H relaxation rates at 20 MHz were also measured on a Minispec Bruker PC-20.

EPR Measurements. EPR Spectra: Bruker ESP-300E spectrometer, operating at 9.43 GHz (0.34 T, X-band). The 5 mm aq. solns. of the complexes were measured at 298 K in a quartz flat cell. Typical parameters used were: sweep width 40 mT, microwave power 20 mW, modulation amplitude 0.32 mT, and time constant 0.02 s. The frequency was calibrated with diphenylpicrylhydrazyl (dpph) and the magnetic field by using Mn²⁺ in MgO.

REFERENCES

- [1] 'The Chemistry of Contrast Agents in Medical Magnetic Resonance Imaging', Ed. A. E. Merbach, É. Tóth, Wiley, Chichester, England, 2001.
- [2] S. C. Chu, M. M. Pike, E. T. Fossel, T. W. Smith, J. A. Balschi, C. S. Springer, *J. Magn. Reson.* **1984**, *56*, 33.
- [3] R. C. Holz, W. deW. Horrocks Jr., *Inorg. Chim. Acta* **1990**, *171*, 193.
- [4] R.-Y. Wang, J.-R. Li, T.-Z. Jin, G.-X. Xu, Z.-Y. Zhou, X.-G. Zhou, *Polyhedron* **1997**, *16*, 1361.
- [5] A. Mondry, P. Starynowicz, *Inorg. Chem.* **1997**, *36*, 1176.
- [6] R. Ruloff, T. Gelbrich, J. Sieler, E. Hoyer, L. Beyer, *Z. Naturforsch., B* **1997**, *52*, 805.
- [7] R. Ruloff, P. Prokop, J. Sieler, E. Hoyer, L. Beyer, *Z. Naturforsch., B* **1996**, *51*, 963.
- [8] S. Aime, A. Barge, A. Borel, M. Botta, S. Chemerisov, A. E. Merbach, U. Müller, D. Pubanz, *Inorg. Chem.* **1997**, *36*, 5104.
- [9] M. Botta, *Eur. J. Inorg. Chem.* **2000**, 399.
- [10] C. F. G. C. Geraldes, A. M. Urbano, M. C. Alpoim, A. D. Sherry, K. T. Kuan, R. Rajagopalan, F. Maton, R. N. Muller, *J. Magn. Reson. Imaging* **1995**, *13*, 401.
- [11] C. F. G. C. Geraldes, A. D. Sherry, W. P. Cacheris, K. T. Kuan, R. D. Brown III., S. H. Koening, M. Spiller, *Magn. Reson. Med.* **1988**, *8*, 191.
- [12] H. Lammers, F. Maton, D. Pubanz, M. W. van Laren, H. van Bekkum, A. E. Merbach, R. N. Muller, J. A. Peters, *Inorg. Chem.* **1997**, *36*, 2527.
- [13] I. Solomon, *Phys. Rev.* **1955**, *99*, 559.
- [14] N. Bloembergen, *J. Chem. Phys.* **1957**, *27*, 572.
- [15] N. Bloembergen, L. O. Morgan, *J. Chem. Phys.* **1961**, *34*, 842.
- [16] J. A. Peters, J. Huskens, D. J. Raber, *Progr. NMR Spectrosc.* **1996**, *28*, 283.
- [17] C. A. Chang, H. G. Brittain, J. Telsler, M. F. Tweedle, *Inorg. Chem.* **1990**, *29*, 4468.
- [18] J. A. Peters, *Inorg. Chem.* **1988**, *27*, 4686.
- [19] C. F. G. C. Geraldes, A. M. Urbano, M. A. Hoefnagel, J. A. Peters, *Inorg. Chem.* **1993**, *32*, 2426.
- [20] M. J. Gueron, *J. Magn. Reson.* **1975**, *19*, 58.
- [21] A. J. Vega, D. Fiat, *Mol. Phys.* **1976**, *31*, 347.
- [22] B. M. Alsaadi, F. J. C. Rossotti, R. J. P. Williams, *J. Chem. Soc., Dalton Trans.* **1980**, 2147.
- [23] B. M. Alsaadi, F. J. C. Rossotti, R. J. P. Williams, *J. Chem. Soc., Dalton Trans.* **1980**, 2151.
- [24] M. S. Nieuwenhuizen, J. A. Peters, A. Sinnema, A. P. G. Kieboom, H. van Bekkum, *J. Am. Chem. Soc.* **1980**, *102*, 12.

- [25] J. H. Freed, *J. Chem. Phys.* **1978**, *68*, 4034.
- [26] D. H. Powell, A. E. Merbach, G. Gonzalez, E. Brücher, K. Micskei, M. F. Ottiviani, K. Köhler, A. von Zelewsky, O. Y. Grinberg, Y. S. Lebedev, *Helv. Chim. Acta* **1993**, *76*, 2129.
- [27] E. Belorisky, P. H. Fries, *Phys. Chem. Chem. Phys.* **2004**, *6*, 2341 and ref. cit. therein.
- [28] X. Zhou, P. Caravan, R. B. Clarkson, P.-O. Westlund, *J. Magn. Reson.* **2004**, *167*, 147.
- [29] L. Vander Elst, A. Sessoye, S. Laurent, R. N. Müller, *Helv. Chim. Acta* **2005**, *88*, 574.
- [30] D. H. Powell, O. M. Ni Dubhgaill, D. Pubanz, L. Helm, Y. S. Lebedev, W. Schlaepfer, A. E. Merbach, *J. Am. Chem. Soc.* **1996**, *118*, 9333.
- [31] A. Borel, L. Helm, A. E. Merbach, *Chem.–Eur. J.* **2001**, *7*, 600.
- [32] J. W. Chen, R. L. Belford, R. B. Clarkson, *J. Phys. Chem. A* **1998**, *102*, 2117.
- [33] J. S. Fritz, R. T. Oliver, D. J. Pietrzyk, *Anal. Chem.* **1958**, *30*, 1111.

Received October 29, 2004